

QUANTIFYING THE IMPACT OF LOCAL DUST STORMS ON MARTIAN ATMOSPHERE USING THE LMD/UK MARS GLOBAL CLIMATE MODEL.

A. El-Said, S.R. Lewis, M.R. Patel, *The Open University, School of Physical Sciences, Walton Hall, Milton Keynes, MK7 6AA*, F. Forget, *Laboratoire de Météorologie Dynamique, IPSL, Paris, France*.

Introduction: The martian atmosphere has an annual cycle of dust, in addition to global storms (Cantor et al., 2001), small-scale lifting such as dust devils, (Balme and Greeley (2006), Fenton et al. (2016)) and mesoscale (Spiga and Lewis, 2010). There are many local and regional storms on scales of ($> 10^2\text{km}^2$) and ($> 10^6\text{km}^2$) respectively. Regional storms have the potential to reach heights of ($\sim 60\text{km}$). The concentrated part of smaller local dust storms tend to operate within the Mars boundary layer ($\sim 10\text{km}$), (Cantor et al. (2001), Petrosyan et al. (2011)), while the surrounding haze can be detected at $\sim 30\text{km}$ using the high resolution images from the Mars Orbiter Camera (MOC) wide camera images of cloud shade length, (Strausberg et al., 2005). Dust opacities for smaller local events tend vary from a diffusive haze to a concentrated local event (0.54-2.13), (Read and Lewis, 2004). We seek to measure the impact of such events to aid in the quantification of reasonable confidence intervals on atmospheric state predictions for the European Space Agency (ESA), MARs Modelling Information Tool for Engineering (MarMITE) tool. The MarMITE tool will use the latest version of the Mars Climate Database (MCD), (Lewis et al. (1999), Forget et al. (2006), Millour et al. (2012)) to produce ensembles of atmospheric state estimates.

We investigate the impact of local dust storms by inserting dust into the UK/LMD Mars Global Climate Model (MGCM). This is achieved by modifying the dust mass mixing ratio and number of dust particle tracers in the MGCM.

The global dust storm observed on Mars in 2001 (MY25) is a well documented event in the literature. We use the existing literature describing the relevant properties of this event to enable us to compose credible experiments for our study, (Cantor et al., 2001), (Strausberg et al., 2005), (Montabone et al., 2015), (Read and Lewis, 2004).

We insert 3 local dust storms into a prescribed area identified by latitude, longitude and altitude over a short period of time:

1. Dust storm 1, location: ($40^\circ - 50^\circ, 130^\circ - 140^\circ$)
Size: $416\text{km} \times 592\text{km} = 2.48 \times 10^5\text{km}^2$.
Altitude: 8.5km.
Time: $L_s = 0.51^\circ - 1.02^\circ$.
2. Dust storm 2 - ($40^\circ - 50^\circ, 130^\circ - 140^\circ$)
Size: $416\text{km} \times 592\text{km} = 2.48 \times 10^5\text{km}^2$.

Altitude: 8.5km.

Time: $L_s = 103.13^\circ - 103.59^\circ$.

3. Dust storm 3 - near Schiaparelli landing site ($0^\circ - 5^\circ, 1^\circ - 4^\circ$):

Size: $295\text{km} \times 296\text{km} = 8.73 \times 10^4\text{km}^2$.

Altitude: 8.5km.

Time: $L_s = 242.04^\circ - 242.69^\circ$.

These properties were selected with the properties of real local dust storms in mind.

The model is run at a resolution of T31, while physical processes are calculated on a grid-box of size $5^\circ \times 5^\circ$. We only transport the dust particle number and mass mixing ratio tracers and keep dust as the only radiatively active scatterer. We use a version of the MGCM where the dust opacities are not scaled to match observations, thus having more freedom to follow the flow. We also ensure that radiatively active dust is turned on and we allow dust to be lifted by surface winds and dust devils.

Twin experiments are performed with a reference run and another run with the dust storms inserted. We then quantify the overall impact of the dust storms by examining the atmospheric temperature, pressure, density, zonal wind velocity, and the incoming and outgoing radiative fluxes.

Dust storm evolution: Here we show the spatial-temporal evolution of dust storm 1. Figure 1 shows differences of q between the dust storm run and the reference run. Areas shaded in red and blue show an increase and decrease in q in the dust storm run over the reference run respectively. This dust storm begins at the beginning of the simulation, $L_s = 0^\circ$, corresponding to the beginning of northern hemisphere spring equinox.

We see the transportation of dust quickly evolve from the point of storm initiation swirling around the upper latitudes for the first few solar longitudes. From $L_s = 4^\circ$ a near-global increase of q can be seen (red) which increases for the next 5 solar longitudes, mostly concentrated in the lower altitude areas. Synchronous to the increase in q , we have an increasingly offsetting reduction (blue) showing a natural circulation of dust continuing across the planet.

An interesting effect seen as soon as the dust storm develops is the reduction of q in the higher altitude regions, Olympus Mons and Tharsis. This effect is seen mostly throughout the mars month in Figure 1. The dust storm rapidly spreads across through the western

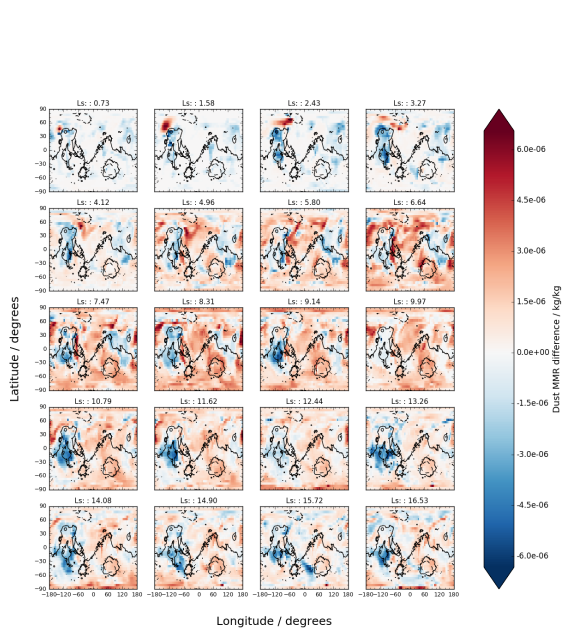


Figure 1: Dust storm 1. Time series of the difference in dust mass mixing ratios ($q = q_{ds} - q_{rr}$) with latitude and longitude at the lowest model level. The Martian topography is shown in black contour lines from the Mars Orbiter Laser Altimeter (MOLA). The top left plot starts at $L_s = 1$ and the temporal progression goes from left to right.

longitudes nearing the central longitudes in the northern hemisphere. The topography plays the role of initially keeping it in the lower altitudes until enough dust lifting has occurred. Figure 2 shows that the simulated runs are not too dissimilar from Mars year 28, while bearing in mind the first half of Mars year 28 was not well observed. The lead-time of the dust storms effects vary. Figure 2(a) shows an increase of dust optical depth across a larger cross-section of latitudes, in comparison to Figure 2(b), for example there is an optical depth haze of about 0.8 extended nearly to the southern ice cap in the first 10 solar longitudes. The second and third dust storms at $L_s = 103^\circ$ and $L_s = 242^\circ$ in Figure 2(a) show small spikes in optical depth at approximately $L_s = 120^\circ$ and $L_s = 252^\circ$ respectively, while also the surrounding lesser haze spreads to more latitudes than in the reference run. The peak optical depth of the dust storm run (Figure 2(a)) is twice as large as the reference run (Figure 2(b)).

We now show the impact of the local dust storms on atmospheric model variables.

Long term local dust storm impact: Here we show the results obtained from examining the temperature and radiative fluxes. In Figure 3 we see the impact of the dust storms on the atmospheric temperature in lowest 5m of the atmosphere. The effects of the dust storms on the temperature are quite minimal. The largest effects are seen about 2 months after the final dust storm. These

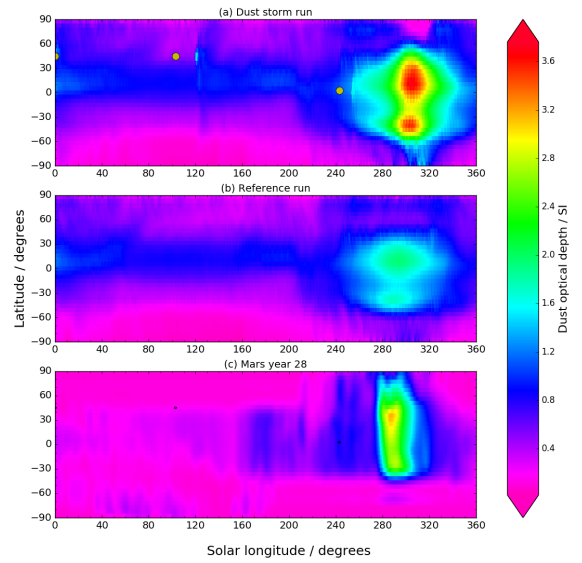


Figure 2: Zonally averaged, temporally averaged over $L_s = 10^\circ$, plot of dust optical depth with latitude against solar longitude. The yellow dots are the latitude points where the storms were inserted. Plot (a) shows the MGCM run where the dust storms were inserted. Plot (b) shows the reference run with no dust storms inserted. Plot (c) shows Mars year 24 obtained from TES observations.

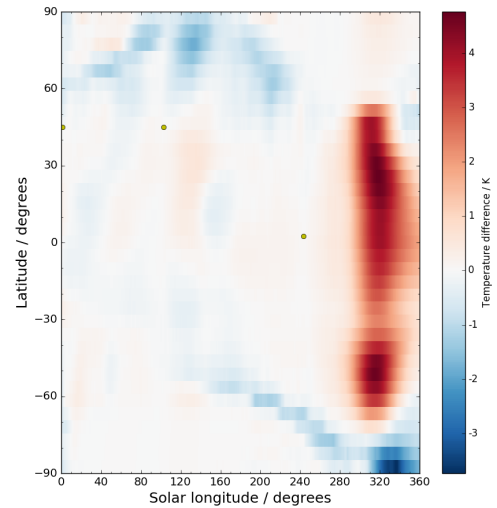


Figure 3: Zonally averaged, temporally averaged over $L_s = 10^\circ$, plot of atmospheric temperature (5m altitude) differences ($T = T_{ds} - T_{rr}$) with latitude and solar longitude. The yellow dots are the points of latitudes at which the dust storms began.

effects coincide with the large optical depth (shown in Figure 2) which occur later in the year. The bigger effect seen between $L_s = 300^\circ - 330^\circ$ may be due to an accumulation of dust from the three inserted dust storms, but it is certainly not as a direct result.

The overall long-term impact caused by the dust storms on the temperature is in the range of $9K$, which is a considerable amount (3 – 5%), considering the average temperature is approximately $170 - 300K$ on Mars.

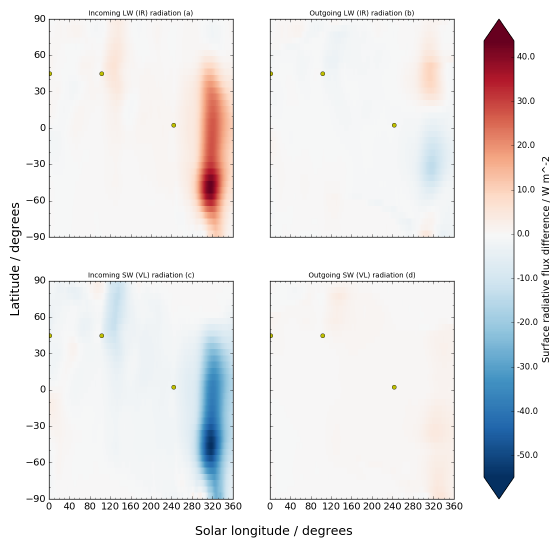


Figure 4: Zonally averaged, temporally averaged over $L_s = 10^\circ$, plot of surface radiative flux differences ($\phi = \phi_{ds} - \phi_{rr}$) with latitude and solar longitude. The surface radiative fluxes are broken down into long wave (infrared) radiation (a) incoming and (b) outgoing, and short wave (visible light) radiation (c) incoming and (d) outgoing with respect to Mars' surface.

In Figure 4 we see abrupt changes in two time periods for the incoming radiative fluxes (SW and LW). The first change radiative fluxes can be seen just after the second dust storm at $L_s = 135^\circ$. The second more obvious change is seen around $L_s = 300 - 360^\circ$ a few months after the final dust storm is inserted. This effect coincides with the high optical depth seen in Figure 5 between $L_s = 280 - 340^\circ$.

The effects on outgoing SW and LW radiative fluxes as shown in Figure 4 are quite minimal in comparison to the incoming SW and LW radiative fluxes. However we can still see in the outgoing LW plot, Figure 4(b), that in the same region of high dust optical depth in Figure 2 at approximately $L_s = 320^\circ$ onwards, there is a small change.

Short term local dust storm impact: Taking a closer look at the more immediate impact of dust storm 3 over a shorter time-period, the change in temperature is almost instantly visible.

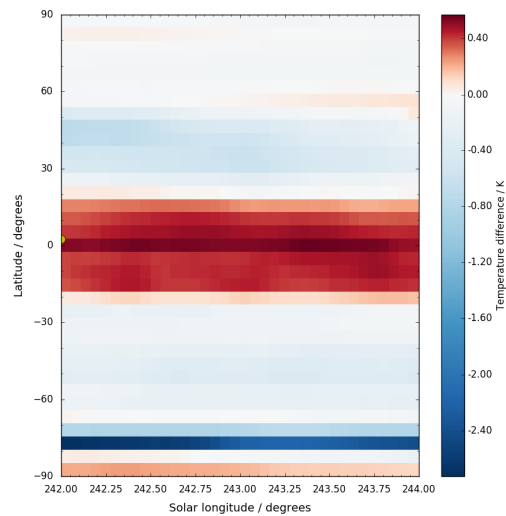


Figure 5: Zonally averaged, temporally averaged over $L_s = 3^\circ$, plot of atmospheric temperature (5m altitude) differences ($T = T_{ds} - T_{rr}$) with latitude and solar longitude. The yellow dot shows the beginning of dust storm 3.

Figure 5 shows immediate effect upon dust storm insertion, with an impact range of $\sim 3K$ over latitudes (20S - 20N). The average temperature in this region in the absence of the dust storm is $169K$, so the immediate impact is just under 2%.

Summary: The first dust storm doesn't have the same effect as the second and third dust storms, mainly due to the time of year. Dust storms have frequently been observed in the second half of the Mars year when the advective properties are more pronounced such as the Hadley cell, (Montabone et al., 2015).

The short term immediate impact of dust storm 3 on the atmospheric temperature in the lower altitudes, 5m off the ground, is just under 2%. The longer-term effects are as a result of the accumulation of the 3 dust storms, which as we see in Figure 2, raises the peak optical depth of the dust storm run to be over double to that of the reference run in Figure 2(b). The overall radiative effect of local dust storms is minimal in general, however as one would expect, there is a visible difference in the temperature and radiative fluxes as a result of the storms.

Future work: Investigating heat rates with the distribution of varying dust particle sizes would be a good next step. Relating the temperature changes to the dust particle distribution would further explain in more detail what we are seeing here. Preliminary results have been obtained for dust distributions in the vertical, however shorter time windows are needed to determine the short-term effects more clearly. Analysing the third dust storm using the LMD Mesoscale model would further explain some of the smaller scale behaviour.

REFERENCES

Acknowledgements: The author gratefully acknowledges the funding granted under the ESA MarMITE

project (contract no: 40001141381115/NL/PA).

References

- Balme, M. and Greeley, R. (2006). Dust devils on earth and mars. *Reviews of Geophysics*, 44(3).
- Cantor, B. A., James, P. B., Caplinger, M., and Wolff, M. J. (2001). Martian dust storms: 1999 mars orbiter camera observations. *Journal of Geophysical Research: Planets*, 106(E10):23653–23687.
- Fenton, L., Reiss, D., Lemmon, M., Marticorena, B., Lewis, S., and Cantor, B. (2016). Orbital Observations of Dust Lofted by Daytime Convective Turbulence. *Space Science Review*.
- Forget, F., Millour, E., Lebonnois, S., Montabone, L., Dadas, K., Lewis, S., Read, P., López-Valverde, M., González-Galindo, F., Montmessin, F., et al. (2006). The new mars climate database.
- Lewis, S. R., Collins, M., Read, P. L., Forget, F., Hourdin, F., Fournier, R., Hourdin, C., Talagrand, O., and Huot, J.-P. (1999). A climate database for mars. *Journal of Geophysical Research*, 104(E10):24–177.
- Millour, E., Forget, F., Spiga, A., Colaitis, A., Navarro, T., Madeleine, J.-B., Chauffray, J.-Y., Montabone, L., Lopez-Valverde, M., Gonzalez-Galindo, F., et al. (2012). Mars climate database version 5.
- Montabone, L., Forget, F., Millour, E., Wilson, R., Lewis, S., Cantor, B., Kass, D., Kleinböhl, A., Lemmon, M., Smith, M., et al. (2015). Eight-year climatology of dust optical depth on mars. *Icarus*, 251:65–95.
- Petrosyan, A., Galperin, B., Larsen, S. E., Lewis, S., Määttänen, A., Read, P., Renno, N., Rogberg, L., Savijärvi, H., Siili, T., et al. (2011). The martian atmospheric boundary layer. *Reviews of Geophysics*, 49(3).
- Read, P. L. and Lewis, S. R. (2004). *The martian climate revisited: Atmosphere and environment of a desert planet*. Springer Science & Business Media.
- Spiga, A. and Lewis, S. R. (2010). Martian mesoscale and microscale wind variability of relevance for dust lifting. *Mars*, 5:146–158.
- Strausberg, M. J., Wang, H., Richardson, M. I., Ewald, S. P., and Toigo, A. D. (2005). Observations of the initiation and evolution of the 2001 mars global dust storm. *Journal of Geophysical Research: Planets*, 110(E2).